EFFECTS OF AXIAL LOADS AND HIGHER ORDER MODES ON THE SEISMIC RESPONSE OF TALL BRIDGE PIERS

E. Tubaldi[1], F. Scozzese[2*], D. De Domenico[3], A. Dall'Asta[2]

[1] Department of Civil and Environmental Engineering, University of Strathclyde, 75 Montrose Street, Glasgow, G1 1XQ, UK
e-mail: enrico.tubaldi@strath.ac.uk

[2] School of Architecture and Design (SAAD), University of Camerino
Viale della Rimembranza, 63100, Ascoli Piceno (AP), Italy
[*] Corresponding author, e-mail: fabrizio.scozzese@unicam.it, andrea.dallasta@unicam.it

[3] Department of Engineering, University of Messina, 98166 S. Agata, Messina, Italy
e-mail: dario.dedomenico@unime.it

Keywords: Tall bridge piers, Axial load effects, Higher order mode effects, Analytical model, Seismic response, Vibrations.

ABSTRACT

Tall piers are essential components of the earthquake resisting system of bridges. The dynamic behaviour of tall piers differs significantly from that of short piers due to a number of factors, such as their high flexibility and inertia. This paper aims to quantify the influence of axial loads and higher order modes on the seismic response of bridges tall piers and to provide results useful for a more informed design and assessment. For this purpose, an analytical formulation of the dynamic problem, developed and validated in a previous study, is employed to analyse a wide range of piers and bridge configurations. In the first part of the paper, a thorough parametric investigation is carried out to evaluate the influence of axial loads and higher order modes on both the modal properties and the seismic response of tall piers with different geometries and vertical loads. Subsequently, three realistic case studies representing bridges with different geometrical, mechanical and dynamic conditions are analysed and seismic time-history analyses are performed to further investigate the problem. The obtained results provide useful insights into the seismic behaviour of bridges with tall piers, identify the relevant governing parameters and shed light on the accuracy of simplified approaches suggested by the Eurocode 8 to account for the second order effects.

1 INTRODUCTION

Many bridges in the world are characterized by the presence of tall piers as part of the earthquake resisting system. The dynamic behaviour of tall piers may be very different from that of short piers due to a number of factors, such as their higher flexibility, the higher ratio between the pier mass and the deck mass they have to withstand, and the influence of the axial loads on the vibrational properties.

The large flexibility of tall piers leads to large values of the fundamental period in the horizontal direction, which in turn results in low seismic response spectral accelerations for the bridge. In this situation, it is not cost-effective nor necessary to resort to seismic isolation or to design the piers for increased ductility [1]-[3]. Therefore, tall piers are usually designed to maintain an elastic (or limitedly ductile) behaviour under seismic actions.

In many design codes, a single-degree-of-freedom (SDOF) approximation of the bridge behaviour is allowed under certain conditions. This is reported, for instance, in Eurocode 8 ("Fundamental mode method" reported in §4.2.2 of EC8-Part 2 [4]), in the AASHTO LRFD bridge design specifications (e.g. in the "Single-Mode Spectral Method" and in the "Uniform Load Method" in §4.7.4.3.2 of [5]), as well as in many national codes such as the recent Italian Building Code NTC-2018 [6]. However, the SDOF model is allowed only if the pier mass is relatively small compared to the deck tributary mass, so that higher order modes have negligible influence on the bridge dynamic behaviour. As an example, according to the EC8 the pier mass does not have to exceed 20% of the tributary mass of the deck. On the contrary, in bridges with tall piers, the high ratio between the pier mass and the deck tributary mass often results in a significant influence of the higher order modes on the seismic response, so that an accurate description of the pier geometry and inertia distribution is strictly required [7]-[11]. Recent results from shake table tests [12] as well as from model-updating hybrid tests [13], [14] on tall-pier models confirmed that the contribution of higher modes may significantly affect the seismic response of tall piers. One important effect is the increase of bending moment demand at pier mid-height, which may trigger additional plastic regions for very high seismic intensities, such as peak ground acceleration (PGA) values higher than 0.8g [12].

Moreover, bridges with tall piers are sensitive to axial loads, which may significantly influence the dynamic properties of the system both in the elastic range [15] and at the collapse conditions [16]-[19]. Thus, the effects of axial loads acting on the deformed bridge configuration need to be included in the analysis by using a geometrical formulation coherent with the range of displacement and rotation of interest (e.g., fully non-linear, moderate rotations, p-delta effects)

[7], [20]. In bridge design practice, the axial-load effects are usually taken into account in a simplified manner by introducing an amplification factor for the pier seismic moments (also called moment magnification) evaluated via first-order analysis, as reported, for instance, in §5.4 of EC8-Part 2 [4], in §4.5.3.2.2b of AASHTO LRFD bridge design specifications [5], and in §7.9.4 of NTC-2018 [6]. The formulations available for the amplification factors are, however, based on simple hysteretic SDOF models [21]-[26], and thus they do not adequately represent the behaviour of tall piers.

Also, the features of the seismic events might affect the response of tall piers, as recently analysed in [27], [28], where the authors observed that near-fault motions generally lead to higher seismic vulnerability for piers with height from 40 to 80 m; such study was performed by analysing the response of a single demand parameter, the curvature ductility demand, and by developing fragility curves for comparing the performances under near fault and far field records.

Recently, an analytical model and a related dimensionless formulation was proposed in [15] to shed light on the main characteristics of the dynamic and seismic behaviour of tall piers vibrating in their linear elastic range, by accounting for both the influence of axial loads and higher order modes. The model also allowed the derivation of an analytical solution for the eigenvalue and the seismic problem by extending previous results for similar problems [29]-[31], in particular by application of the Frobenius method [31]. The reliability of the results achieved through the adoption of such analytical formulation was also assessed and the proposed model and the related kinematic assumptions were validated in [15] by comparison with a large displacement formulation approach.

The present study builds on this work and aims at exploiting the formulation developed in [15] in an extensive parametric analysis aiming to achieve the following main objectives:

1. evaluating the influence of higher order modes and axial load effects on the seismic response of tall piers for different values of the characteristic parameters identified in [15] varying in a range of practical interest;
2. evaluating whether and to which extent the use of the amplification factor suggested by EC8-Part 2 overestimates the seismic demand;
3. providing results useful for a more informed design and assessment of the seismic response of tall piers by accounting for the influence of higher modes and second order effects.

In the second part of the paper, three realistic piers with different geometrical and mechanical properties and corresponding to different values of the characteristic non-dimensional parameters are selected and analysed, to reinforce the findings of the parametric analyses and better explain the implications on the assessment and design of bridges with tall piers.

2 ANALYTICAL PROBLEM FORMULATION AND SOLUTION

In this section, the analytical formulation developed in [15] and used for the purposes of the present study is briefly recalled. This formulation is based on a continuous modelling approach for the tall pier (Fig. 1), which consists of a linear-elastic Euler-Bernoulli cantilever beam with bending stiffness $b(x)$, mass per unit length $m(x)$, and tip mass M_T at the top, with $x \in [0, H]$. The formulation describes the perturbed motion starting from a reference configuration (Fig. 1-a) where the beam axis lies over the x-axis; the beam is subjected to a concentrated compression force, P, at the free end, and to a distributed compressive load, $m(x)g$, along its height. The term P describes the vertical force related to the weight sustained by the pier supports, whereas the term M_T represents the mass associated to the horizontal inertial forces and depends on the static scheme of the deck in the horizontal plane. It is worth noting that the tip mass at the pier top M_T and the deck vertical reaction P are two independent parameters, differently from mass and weight of the pier which are, instead, related through the acceleration of gravity and can thus be described by a single parameter. The proposed model is consistent with the "Individual pier" modelling approach according to §4.2.2.6 of EC8-Part 2 [4], and it can be employed to describe the seismic longitudinal and transversal behaviour of piers under some regularity conditions that allow to consider a single pier with the tributary deck mass to represent the whole bridge; for example, under the transverse seismic input the model is suitable for the case in which there is no significant interaction between the adjacent piers (e.g., long and/or transversally flexible decks).

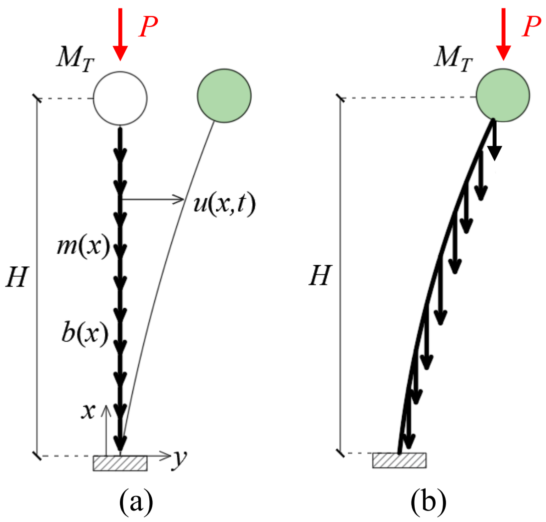

Fig. 1. a) Pier model and undeformed configuration; b) deformed pier configuration.

The formulation developed in [15] describes the infinitesimal perturbed motion of the continuous system in the neighbourhood of the axially loaded reference configuration, under the hypothesis of small strains and displacements, and linear elastic behaviour of the pier. It is noteworthy that these assumptions are valid for most of tall piers, which are characterized by a long vibration period such that the inelastic behaviour of the system is activated only for very high seismic intensities (for example, in the shaking-table experiments of [12], the first plastic hinge at the pier base formed for PGA>0.6g and the one at mid height was observed for PGA levels higher than 0.8g). Under these assumptions, it is possible to define vibration modes of the system, even though these are influenced by axial load effects, and thus the response to the seismic input can be expressed by superimposing the contribution of the various modes.

In [15], the following analytical expression of the circular frequency for the *s*-th vibration was derived:

$$\omega_s^2 = \frac{\mathcal{K}(\psi_s,\psi_s) - \mathcal{N}(\psi_s,\psi_s)}{\mathcal{M}(\psi_s,\psi_s)} = \frac{\bar{k}_s}{\bar{m}_s} \tag{1}$$

where $\bar{k}_s$ and $\bar{m}_s$ are the generalized stiffness and mass of the *s*-th mode, whose shape is described by Ψ_s, a spatial function representing the *s*-th mode shape and belonging to the space U of transverse displacement functions satisfying the essential boundary conditions; $\mathcal{K}$, $\mathcal{N}$, $\mathcal{M}$ are bilinear symmetric forms mapping pairs of functions belonging to U into the space $\mathcal{R}$ of real numbers. The expression of $\bar{k}_s$ considers the reduction of stiffness due to the so-called P-delta effects.

The dynamic properties of the system are also described by the modal participation factor, ρ_s, and by the modal mass participation factor, MPF_s, defined as follows, respectively:

$$\rho_s = \frac{\mathcal{M}^*(\psi_s)}{\mathcal{M}(\psi_s,\psi_s)} = \frac{\int_0^H m(x)\psi_s(x)dx + M_T\psi_s(H)}{\int_0^H m(x)\psi_s^2(x)dx + M_T\psi_s^2(H)} \tag{2}$$

$$MPF_s = \frac{\left[\mathcal{M}^*(\psi_s)\right]^2}{\mathcal{M}(\psi_s,\psi_s)} \tag{3}$$

According to the mode superposition method, the motion is expressed by the following summation series:

$$u(x,t) = \sum_{s=1}^{\infty}\psi_s(x)q_s(t) \tag{4}$$

where $q_s(t):[t_0,t_1]\rightarrow R$ is the generalized coordinate corresponding to Ψ_s.

The s-th decoupled equation for $q_s(t)$, obtained by employing the orthogonality conditions and by adding a source of inherent damping, reads as follows:

$$\ddot{q}_s(t)+2\xi_s\omega_s\dot{q}_s(t)+\omega_s^2 q_s(t)=-\rho_s\ddot{u}_g(t) \tag{5}$$

where ω_s^2 is the circular frequency whose expression is given in Equation (1), ξ_s is the s-th mode damping factor, and ρ_s is the s-th mode participation factor. The values of ξ_s for the various vibration modes can be calibrated based on experimental observations [32].

Once the displacement response history is evaluated, the histories of the bending moment and of the shear along the beam can be obtained as follows:

$$M(x,t)=-b(x)u''(x,t)=-b(x)\sum_{s=1}^{\infty}\psi_s''(x)\cdot q_s(t) \tag{6}$$

$$V(x,t)=\left[-b(x)u''(x,t)\right]'-N(x)u'(x,t)=-\sum_{s=1}^{\infty}\left\{\left[b(x)\psi_s''(x)\right]'+N(x)\psi_s'(x)\right\}q_s(t) \tag{7}$$

3 PARAMETRIC STUDY

In this section, the characteristic parameters controlling the problem are first introduced. Then, the influence of higher order modes on the pier dynamic behaviour is analysed by considering the relation between the characteristic parameters and the modal properties. Successively, a parametric study is carried out to evaluate the influence of higher order modes and axial load effects on the seismic response.

3.1 Characteristic parameters

Under the assumption of homogeneous pier mass and stiffness (i.e., $m(x)$=m and $b(x)$= EI), the internal compressive action simplifies to $N(x) = P + m(H-x)$ and the characteristic non-dimensional parameters controlling the dynamic behaviour of the system in Fig. 1, evaluated by applying the Buckingham's Pi-theorem, are only three [15], namely:

$$\alpha^2=\frac{P}{P_{cr}}=\frac{P\cdot 4H^2}{\pi^2 EI},\quad \beta=\frac{\bar{m}H}{M_T},\quad \gamma=\frac{\bar{m}gH}{P_{cr}}=\frac{\bar{m}gH\cdot 4H^2}{\pi^2 EI} \tag{8}$$

Parameter α^2 represents the ratio between the load at the pier top (deck reaction), P, and the Euler buckling load, P_{cr}, of a cantilever beam loaded by a concentrated force at its top. Parameter γ denotes the ratio between the total pier weight $\bar{m}gH$ and P_{cr}. Thus, the sum α^2+

γ provides a non-dimensional measure of the total vertical loads acting on the pier in relation to the buckling load and expresses the propensity to second order effects, so that the adjective "slender" can be attributed to piers for which $\alpha^2+\gamma$ is significantly larger than 0 (conversely, stocky piers are characterized by low $\alpha^2+\gamma$ values). Finally, β describes the ratio between the distributed pier mass and the top concentrated mass M_T. It is noteworthy that in the particular case of $P=M_T g$ one has $\gamma=\beta\alpha^2$, hence the problem is governed by two parameters only, whereas in the case of zero distributed mass $\beta = \gamma = 0$ and the problem is governed by a single parameter.

While the modal properties of the system depend only on these non-dimensional parameters, the response to a seismic input also depends on the system fundamental vibration period. This can be described by $T_0=\dfrac{2\pi}{\omega_0}$, where ω_0 is the circular frequency of the pier obtained by neglecting the distributed mass and the axial load effects, i.e.:

$$\omega_0=\sqrt{\frac{3EI}{M_T H^3}} \tag{9}$$

In this study, the values assumed for the pier characteristic parameters are chosen to cover a wide range of behaviours typical of real bridge configurations.

The parameter α^2 is varied between 0.01 and 0.4. Higher values are not considered because they would result in piers close to buckle under the non-seismic load combinations.

The values assumed for β are in the range between 0.01 and 3. The lower limit corresponds to a pier with a negligible mass compared to the mass at its top, whereas the higher limit corresponds to a very high pier mass and a low mass at the pier top. This situation is typical of piers that are disconnected by the deck through a sliding bearing at their top.

In order to limit the parameters to be varied in the parametric study, it is assumed that $\gamma=\beta\alpha^2$.

The period T_0 is assumed to vary in the range between 3s and 8s. Lower vibration periods are not considered because they would correspond to short piers, which are expected to exhibit an elastoplastic behaviour, not considered by the model. On the other hand, vibration periods higher than 8.0 s are not considered, because they would correspond to very slender piers, whose response may be more affected by loads different from the seismic loads (e.g., wind).

3.2 Modal properties

The ratio between the *i*-th circular frequency of the pier, ω_i, and ω_0, can be expressed in terms of a non-dimensional frequency ratio as:

$$\frac{\omega_i}{\omega_0} = f\left(\alpha^2, \beta, \gamma\right) \tag{10}$$

It can be shown that also the modal shapes and other modal properties (e.g., the modal participation factors) depend only on the three identified non-dimensional parameters.

In [15], the relation between the non-dimensional parameters and the modal properties of the system was investigated and the study outcomes can be synthesized as follows: the circular frequencies of the system decrease with increasing α^2 and the axial load significantly affects only the fundamental circular frequency, whereas the circular frequency of the higher modes are weakly sensitive to variations of α^2. The study is herein extended to assess the influence of the axial loads on the modal participating mass, which is a useful parameter providing direct information on the contribution of the vibration modes to the total base shear of the system; in fact, in the case of unit base acceleration, the base shear is exactly equal to the sum of all modal participating masses in a given direction [33]. To this aim,

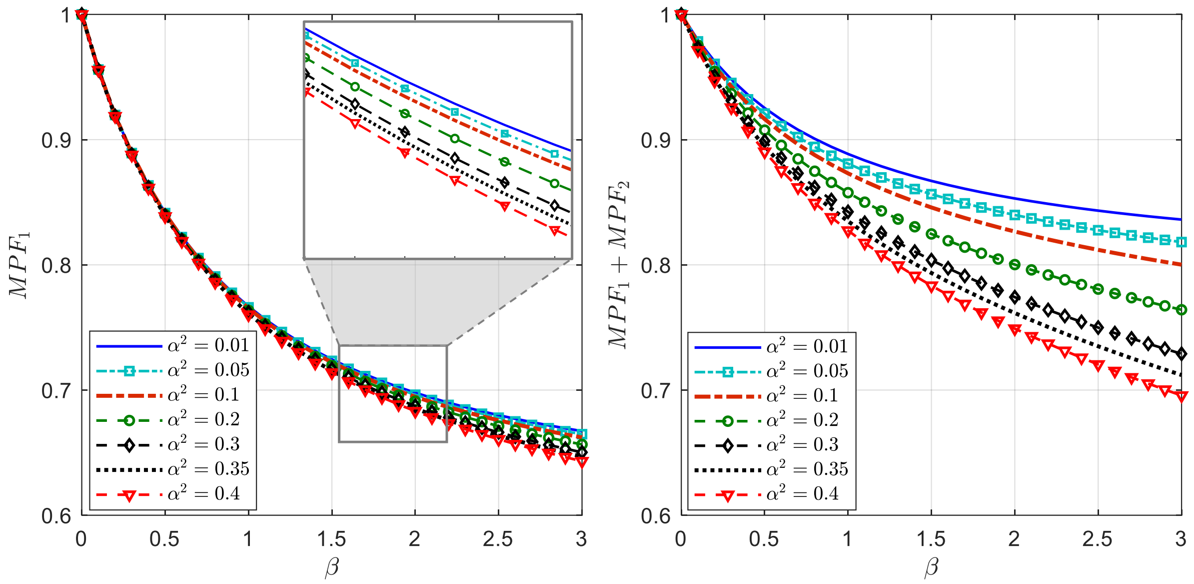

Fig. 2 plots the variation with α^2 and β of the first modal participating mass, MPF_1, and of the sum of the first two participating masses $MPF_1 + MPF_2$, normalized with respect to the total mass of the system, M_{tot}.

In general, these modal properties are equal to 1 in the case of zero pier mass, i.e., for $\beta = 0$ (corresponding to one vibration mode only) and decrease for increasing β values (i.e., increasing pier mass) due to the increase of the higher modes' contribution to the pier motion. Furthermore, the first mode contribution is very high and reaches values higher than 65% for any β value, whereas the contribution of the first two modes is higher than 70% for any combination of β and α^2 value considered. Finally, it is noted that these two modal properties are affected by axial load effects. In particular, the first modal participating mass MPF_1 is almost unaffected by the axial load effects, whereas the second modal participating mass (and hence the sum $MPF_1 + MPF_2$) is reduced from 85% to 70% by increasing the load at the pier top through the α^2 value.

Considering these results, it can be stated that high values of β are a necessary condition for having a contribution of higher order modes to the response, and that for $\beta = 0$, the system behaves as a single degree of freedom system. In most cases, high values of β are also a sufficient condition for higher order modes contribution, but in some particular situations (e.g., extremely rigid piers) the system moves with the ground and thus higher order modes become less important. These special cases can be accounted for by also analysing the parameters α^2 and γ, which attain values close to zeros when the pier's stiffness is very high.

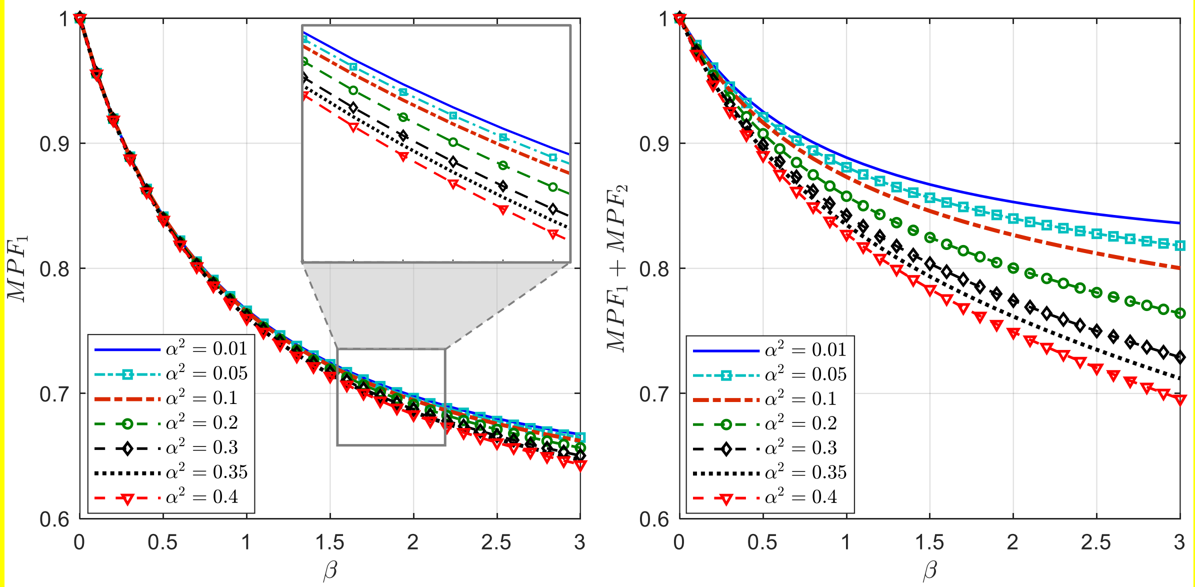

Fig. 2. Plot of the normalized (by the total mass $M_{tot.}$) values of MPF_1 (a) and of the sum $MPF_1 + MPF_2$ (b) vs. β, for different α^2 values.

3.3 Seismic response

In this subsection, a parametric study is carried out to evaluate the influence of axial load effects on the seismic response of tall piers with various geometrical and mechanical properties. The seismic input considered for all the combinations of the above parameters is described by the

EC8 type I soil type B spectrum (soil factor $S = 1.20$), for an importance factor $\gamma_I = 1$ and a peak ground acceleration PGA = 0.30g (Fig. 3). The shape and amplitude of the spectrum at long periods is controlled by the corner period $T_D = 2$s, identifying the beginning of the maximum spectral displacement (MSD) plateau, by the period $T_E = 5$s, corresponding to the end of the plateau and the beginning of the linear decreasing branch of the spectrum, and by the period T_F=10s, beyond which the spectral displacement tends to a constant value (ground displacement d_g). Appendix A of EC8-Part 1 provides the expressions for the displacement spectrum ordinates for periods T>T_E.

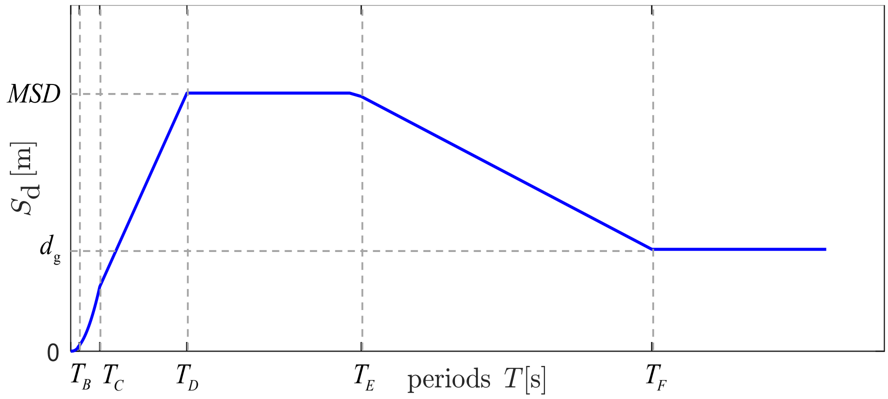

Fig. 3. Displacement response spectrum as per EC8 Part 1 [4] (MSD: maximum spectral displacement).

In the parametric study, three different values of T_0 are considered (consistent with the fundamental periods of the piers analysed in Section 4), corresponding to the ratios $T_0/T_E = 0.6$, 1, and 1.4. The period elongation due to axial load effects and the higher order modes are expected to have a different effect on the systems corresponding to these periods. Seven natural ground motion records compatible with this displacement response spectrum have been selected through the software tool Rexel-Disp [34], which is the result of many recent studies focused on the characterization of ground motions for the seismic design and assessment of long-period structures. The structural response quantities considered are the average values (among the seven excitation scenarios) of the peak transverse displacement at the pier top, of the peak base shear and of the peak bending moment.

In order to shed light on the influence of axial load effects, the ratio between the values assumed by these quantities by accounting for and by disregarding axial load effects are evaluated. These ratios are denoted as r_d, r_V, r_M, and refer to the pier top displacement, to the base shear, and to the base bending moment, respectively. The base bending moment is also evaluated in compliance with the EC8-Part 2 provisions [4], i.e. by increasing the bending moment obtained by a first-order analysis (neglecting axial force contribution) through the moment magnification factor $\Delta M = \frac{1+q}{2} d_{Ed} N_{Ed}$, where N_{Ed} is the axial force, d_{Ed} is the relative transverse displacement of the ends of the member, and q is the behaviour factor considered for the design. A similar moment magnification factor is prescribed also in the Italian building code NTC2018 [6], expressed as $\Delta M = d_{Ed} N_{Ed}$, which thus coincides with the previous one if q=1 (no ductile behaviour).

Therefore, a fourth response ratio r_{MC} is considered in this parametric study as the ratio between the code-based bending moment at the pier base calculated as per the EC8-Part 2 provisions (assuming q=1) and the base bending moment obtained by the proposed formulation, in order to evaluate the accuracy of the EC8 approach.

Fig. 4 reports the values assumed by the ratios r_d and r_V for different values of α^2 and of β varying in the previously identified range and for T_0/T_E = 0.6, 1, and 1.4. Based on these results, it is noted that for all the examined periods the pier top displacement response decreases when the axial load effects are taken into account, since values $r_d < 1$ are obtained for all the combinations of α^2 and β different from zero. More specifically, the top displacement response is reduced up to 30% for combination of shorter periods T_0/T_E = 0.6 and large distributed pier mass compared to the top concentrated mass ($\beta = 3$). However, while the influence of the pier top load (α^2 parameter) is qualitatively similar for the examined periods (both short and long), the displacement response is sensitive to the pier mass distribution only in the relatively short period range (T_0/T_E = 0.6 and 1.0) and is negligible for periods lying in the linear decreasing branch of the spectrum (as in the case T_0/T_E = 1.4). Also, the base shear response, like the pier top displacement response, is reduced if the axial load effects are taken into account. However, in contrast to the displacement response, the greatest reductions effects of base shear are observed for lower values (rather than for higher values) of β. This is related to the fact that the shear demand is significantly influenced by higher order modes, whose relative contribution gets higher for larger distributed pier mass, which is in line with the results presented in the previous paper [15]. In particular, it is observed that values of relatively large distributed pier mass (say $\beta > 0.5$) compensate for the reduction of the shear demand caused by the axial load effects so that the shear response ratio r_V keeps in the neighbourhood of the unity for all the range of α^2 values examined. Overall, the variation of the base shear demand is dramatically influenced by the distributed pier mass when higher axial loads are considered (say in the range $\alpha^2 > 0.2$). In the extreme case of $\alpha^2 = 0.4$ the base shear is reduced up to more than 40% (compared to the case disregarding the axial load effects) for all the three considered periods when the mass is entirely concentrated at the pier top and not distributed along the pier ($\beta \approx 0$). Instead, in the same extreme situation the increase of β would considerably mitigate base shear reductions. These cases are useful to illustrate the importance of axial load effects (related to α^2) and higher order modes (related to β) on the base shear demand of tall piers.

Fig. 5 reports the values assumed by the ratios r_M and r_{MC} for different values of α^2 and of β varying in the previously identified range and for T_0/T_E = 0.6, 1, and 1.4. The qualitative trends of base bending moment ratio r_M follow those of the base shear ratio r_V. This is reasonable since base shear and bending moment response are similarly affected by axial load effects and by higher mode effects. In particular, the increase of the pier top load generates a decrease of the bending moment response ratio (up to 20% in the extreme case $\alpha^2 = 0.4$ and $\beta \approx 0$), whereas the increase of the pier distributed mass compensates for this reduction and may also produce an increment of the base bending moment response (e.g., case of T_0/T_E = 1.4 in Fig. 5c).

It is also interesting to observe that using the EC8-Part 2 formula to account for second order effects (assuming q=1) yields to a significant overestimation of the bending moment demand, compared to the values obtained with the proposed formulation. The highest overestimations (i.e., r_{MC} values) are observed for structural systems with high top loads (large α^2) and negligible distributed mass (low β), which are characterized by r_{MC} values up to 70%. This means that the base bending moment obtained by the simplified EC8 approach is overestimated by more than 70% in comparison to that obtained with the proposed model. This is especially true for larger periods (e.g., T_0/T_E = 1, and 1.4).

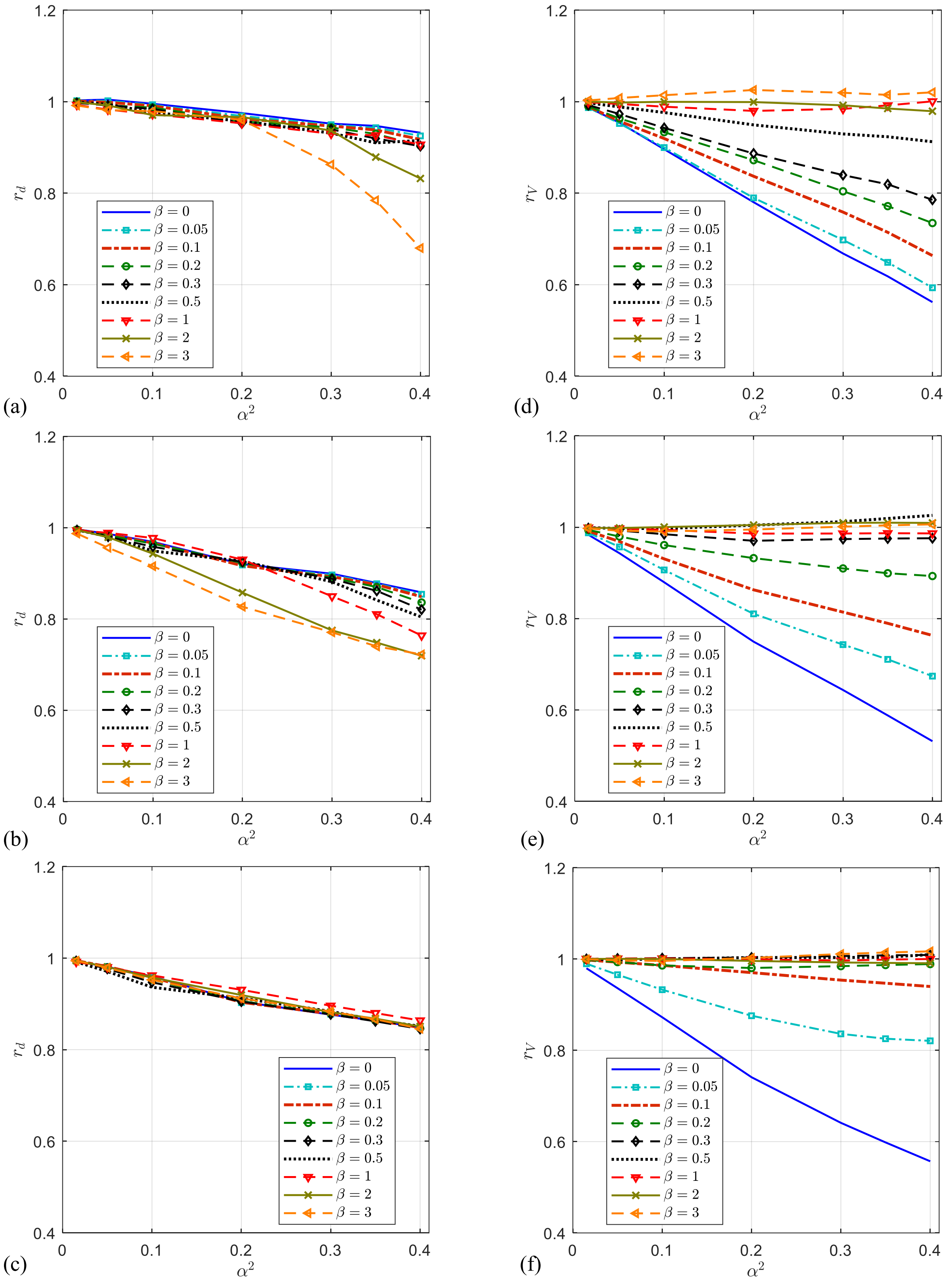

Fig. 4. Variation with α^2 and β of r_d for $T_0/T_E = 0.6$ (a), 1 (b), and 1.4 (c) and of r_V for $T_0/T_E = 0.6$ (d), 1 (e), and 1.4 (f).

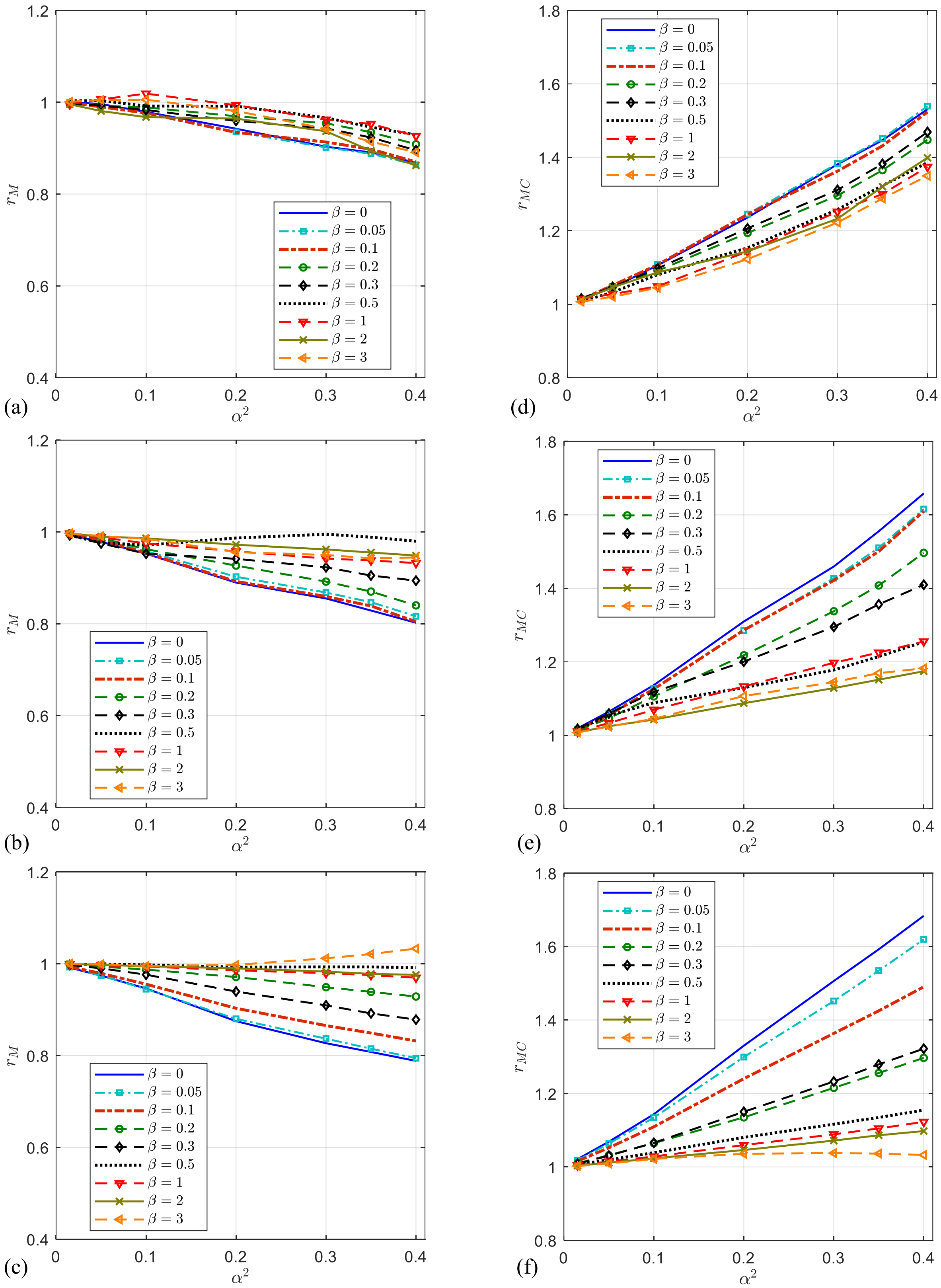

Fig. 5. Variation with α^2 and β of r_M for $T_0/T_E = 0.6$ (a), 1 (b), and 1.4 (c) and of r_{MC} for $T_0/T_E = 0.6$ (d), 1 (e), and 1.4 (f).

On the other hand, the discrepancy between the EC8 approach and the proposed formulation decreases when the pier distributed mass increases (higher β). As an example, for β approaching 3 and for the extreme case of $\alpha^2 = 0.4$, the overestimation reduces to around 30%, 20% and 5%, respectively for the three considered periods T_0 / T_E = 0.6, 1, and 1.4. Thus, the higher the stiffness of the system, the higher the overestimation. In all the cases investigated, the amplification factors of EC8 leads to conservative estimates of the bending moments.

4 CASE STUDIES

In this section, the proposed analysis technique is employed to evaluate the influence of axial load effects and higher order modes on the seismic response of three case studies of tall piers belonging to realistic bridge models taken from the literature.

The main geometrical and mechanical characteristics of the three considered case studies are summarized in the sketch of Fig. 6. In particular, a tall pier taken from Kolias [1], a stockier pier taken from Wei et al. [26] and a very tall pier taken from Li et al. [35] are analysed. The three piers are characterized by different combinations of parameters α^2, β, γ, as reported in Fig. 6, which are representative of different design scenarios discussed in the parametric study above and are thus selected to cover a wide range of bridge configurations and seismic behaviours. In this manner, it is possible to scrutinize the influence of the axial load effects and of the higher order mode effects depending on the different mass and stiffness characteristics of the piers of these three examples.

The seismic input is the same as that employed for the parametric study, i.e., based on the EC8 type I soil type B spectrum soil and a PGA = 0.3 g. Fig. 7 shows the acceleration-displacement response spectrum (ADRS spectrum) of the spectrum-compatible records and of the mean spectrum. The plot in Fig. 7-b provides important information regarding the effect of the modal vibration periods and of the changes due to axial load effect on the seismic demand and it is useful to explain the results of the following seismic analyses. In particular, the axial loads effect in terms of period elongations can be also appreciated.

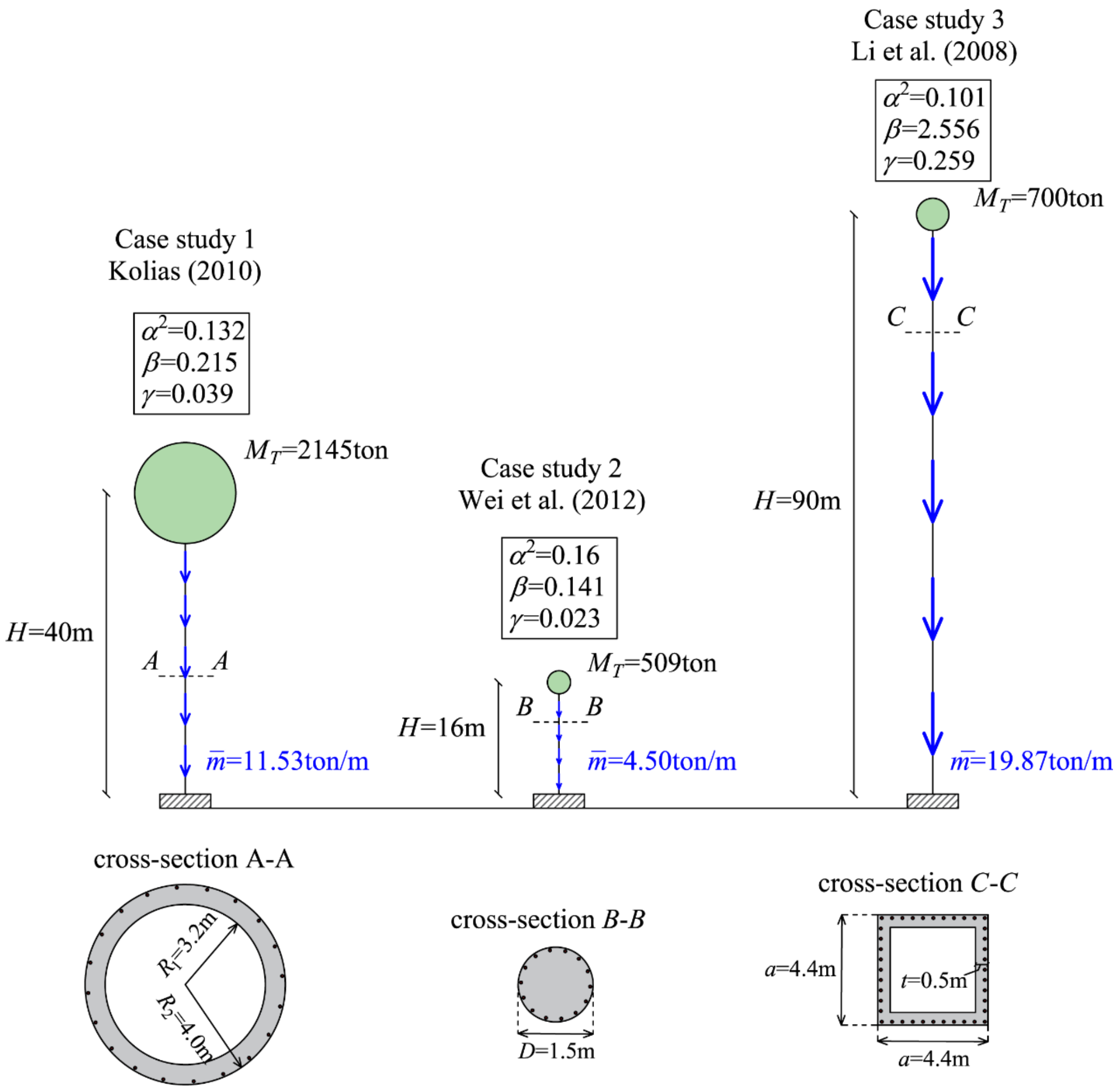

Fig. 6 Sketch of the three case studies analysed in this paper, with different geometrical and mechanical properties.

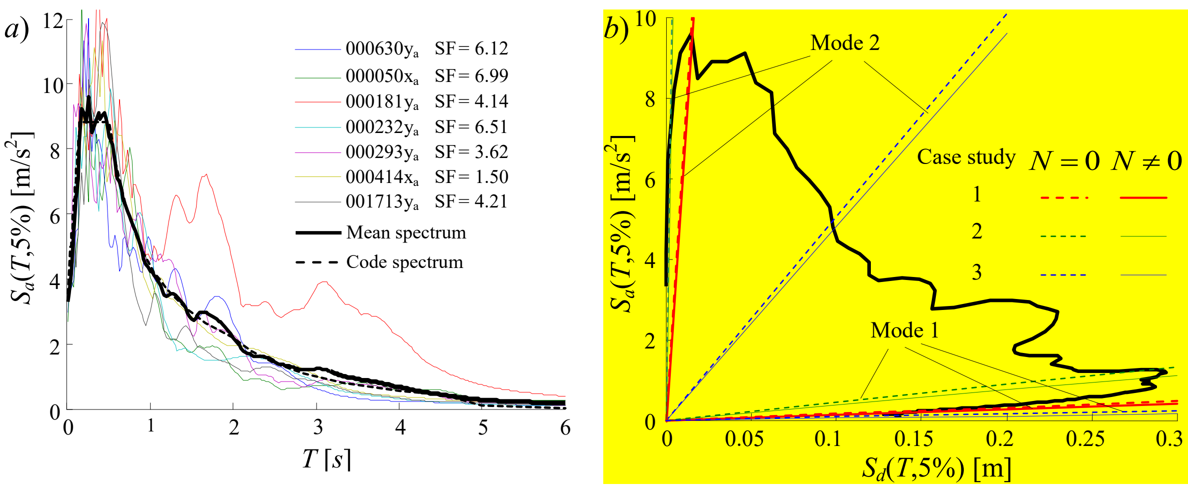

Fig. 7 (a) Acceleration response spectra of natural records and (b) mean ADRS response spectrum with identification of the first two vibration periods of the three case studies analysed below.

4.1 Case study 1 (T_0=5s, $T_0/T_E \approx 1$)

This case study consists of a tall pier belonging to a bridge, whose properties are taken from [1]. The bridge has a three-span steel-concrete composite deck (with span length of 60 m+80 m+60 m) and two identical RC piers. These two piers, of height H = 40 m, have a circular hollow transverse section with external diameter of 4.0 m and internal diameter of 3.2 m. The pier head has a rectangular transverse section with dimensions 4.0 m x 8.0 m, and is 1.5 m high. Class C35/45 concrete is adopted for concrete, and S500 steel grade is used for the longitudinal rebars, with a reinforcement ratio equal to 1.5% of the cross-section area [1].

The formulation described in Section 2 is used to analyse the longitudinal bridge response. Assuming a rigid deck behaviour in line with § 4.2.2.3 of EC8-Part 2 provisions [4], only the response of a single pier is investigated, benefitting from the problem symmetry. The pier effective stiffness accounting for concrete cracking is EI = 7.3086·10^7 kNm^2, whereas the pier distributed mass is $\overline{m} = 11.53$ ton/m. The mass concentrated at the pier top and describing the deck and pier head inertia is M_T = 2145 ton. Since the cross section is uniform along the pier length, the axial force is a linear function $N(x) = P + \overline{m}g(H-x)$ with P = 15470 kN, the pier height H = 40m and the pier mass $\overline{m}H = 461.2$ ton. It is worth noting that in this case study M_T is different from P/g= 1576 ton, because the longitudinal inertial force is resisted by the two piers only, whereas the vertical weight is distributed among the piers and the abutments.

The buckling load of a cantilever beam with the same flexural stiffness of the pier is $P_{cr} = \pi^2 EI/4H^2$ = 1.17·10^8 kN. This corresponds to a ratio $\alpha^2 = P/P_{cr}$ = 0.132. The other two characteristic parameters, related to the distributed mass, have the following values: β = 0.215 and γ = 0.039.

The Frobenius method is applied to solve the eigenvalue problem. The first three longitudinal vibration periods of the pier in the longitudinal direction disregarding axial load effects are 5.003s, 0.251s, and 0.078s. A comparison between the modal vibration periods T_i and mass participating factors MPF_i obtained by accounting for and by disregarding axial load effects (corresponding to assuming $N(x)$ = 0 in Equation (2)) are reported in Table 1.

By inspection of the results listed in Table 1, it can be noticed that only the first vibration mode is significantly affected by the axial load effects. This is expected from the results of the parametric study of the eigenvalue problem discussed in Section 3.2 and also reported in [15]. As an opposite trend, the discrepancies in terms of *MPF*s between the model with and without axial load effects increase for increasing mode order.

The pier seismic behaviour is evaluated by computing, for each of the 7 response-spectrum-compatible records representing the seismic input, the response envelopes (i.e., the peak absolute values) of the displacements, bending moments and shear observed along the pier. Fig. 8 reports the average response obtained from all the considered records, i.e., the average peak values of the displacement $u_{max}(x)$, bending moment, $M_{max}(x)$, and shear, $V_{max}(x)$ for each location x along the pier length.

Table 1. Second-order effects on periods and mass participating factors.

	T_i [s]		MPF_i [%]	
Mode	w/o axial load	w/ axial load	w/o axial load	w/ axial load
1	5.003	5.402	91.491	91.462
2	0.251	0.253	4.966	4.548
3	0.078	0.078	1.249	1.412
4	0.038	0.038	0.767	0.677
5	0.022	0.022	0.345	0.398
6	0.014	0.014	0.297	0.259

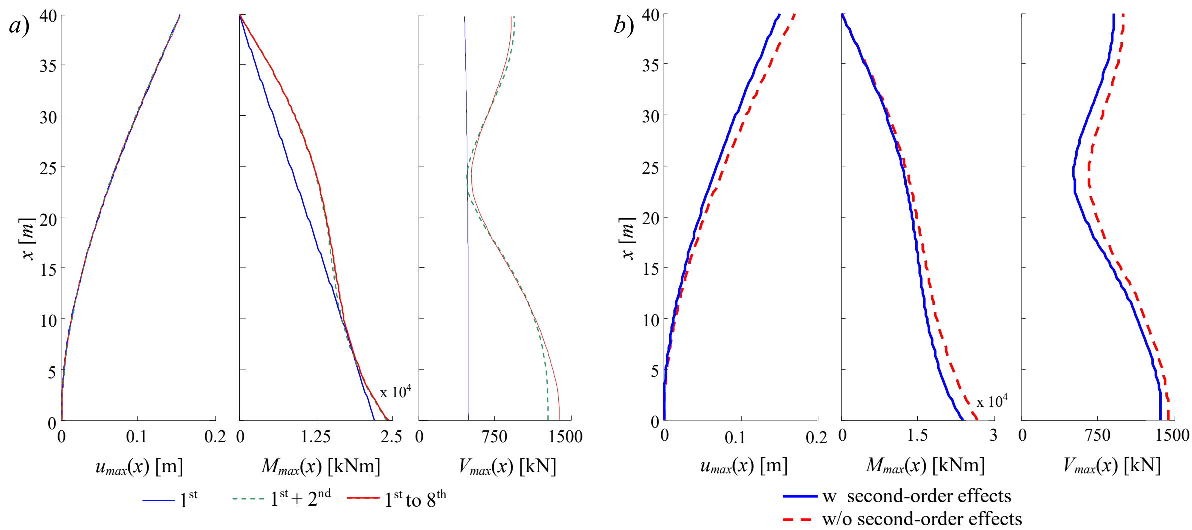

Fig. 8 Average seismic response of case study 1: a) modal contributions to the displacements, bending moments and shear, b) axial load effects on displacements, bending moments and shear profiles.

In particular, Fig. 8-a analyses the contribution of different modes to the seismic response: a comparison of the response envelopes obtained by truncated models that consider the contributions of mode 1, of modes 1 and 2, and of the first 8 modes in terms of displacements, bending moments and shear is illustrated. It is worth noting that the higher modes, related to the mass distributed along the pier, do not considerably influence the displacements, whereas they play a key role in the profiles of both the bending moment and shear force along the pier. It can be seen that the higher mode contribution to the shear demand at the base and at the top of the pier is significant. More specifically, the second-mode contribution significantly affects such shear demand at the two pier ends, as can be seen by comparing the response obtained by including the first two modes with that obtained by including eight modes. Moreover, the shear demand calculated by the first mode only would be largely underestimated.

Fig. 8-b compares the profiles of peak displacement, bending moment and shear force evaluated by the proposed formulation against the corresponding results obtained by neglecting the axial load effects. Notable differences can be observed for all the considered response quantities. Unlike what occurs in static problems, the axial load effects give rise to lower seismic response values along the whole pier height. This result can be explained in view of the fundamental vibration period elongation caused by the additional axial loads, which shifts the structural response on regions of the response spectrum with a lower spectral acceleration (cf. the ADRS response spectrum in Fig. 7-b). As an example, the average peak bending moment value at the base of the pier is 26904 kNm by disregarding axial loads and reduces to the value of 23923 kNm if axial loads are taken into account. Following the EC8-Part 2 approach [4], an amplification of 2475 kNm would be required, corresponding to a ratio r_{MC}=1.22 between the amplified first order base moment and the base moment resulting from the analysis accounting for second order effects. It is observed how this r_{MC} value is very close to the value of r_{MC}=1.19 resulting from the parametric study of section 3.3 (see Fig. 5-e for $\alpha^2 = 0.132$ and $\beta = 0.215$). The slight difference between these two ratios can be attributed to the different values of the characteristic parameter γ, i.e., $\gamma = 0.039$ in the present analysis and $\gamma = \beta\alpha^2 = 0.028$ in the parametric study. This demonstrates the validity and usefulness of the above parametric study for a more informative assessment of the bridge response including axial loads and higher mode effects. Moreover, it is worth noting that in this case the bending moment reduction due to the axial load effect is in net contrast to the amplification obtained by applying the EC8-Part 2 approach [4].

For what concerns the shear demand, the corresponding reduction is a bit less marked than those observed in other response parameters. This is due to the significant influence of higher order modes on the shear force of this pier, and the almost negligible influence of axial load effects on modes of order higher than one.

4.2 Case study 2 (T_0=3s, $T_0/T_E \approx 0.6$)

This section reports the results of the application of the proposed analysis technique to a bridge pier model taken from Wei et al. [26]. The reinforced concrete pier has geometrical properties significantly different from those of the first case study. Its height is H = 16 m, and the cross section is circular with diameter D = 1.5 m. The concrete has cylindrical mean strength of 35 MPa and the steel employed for the longitudinal rebars has strength of 470 MPa. The vertical force at the pier top transmitted by the deck is equal to 5000 kN. The pier stiffness and distributed mass are respectively $b(x) = EI = 3.185 \cdot 10^6$ kNm^2 and $m(x) = \bar{m} = 4.50$ ton/m, whereas the mass concentrated at the pier top is M_T = 509.68 ton. The value of the buckling load of a cantilever beam with the same flexural stiffness of the pier is $P_{cr} = \pi^2 EI/4H^2$ =30692.9 kN, corresponding to a ratio $\alpha^2 = P/P_{cr}$ = 0.1629, very similar to the value obtained for case study 1 despite the different geometry. The values of the other characteristic parameters are β = 0.141, and γ = 0.023. The first three vibration periods of the pier disregarding axial load effects are 2.986s, 0.123s, 0.0382s, whereas the corresponding values obtained by accounting for axial load effects are 3.273s, 0.124s, 0.0383s. As observed for the previous case study, axial load effects influence significantly only the first vibration period. The mass participation factors of the first three modes obtained by accounting for and by disregarding axial loads effects almost coincide and their values are 94.02%, 3.18%, and 0.1%.

Fig. 9-a shows the average of the peak absolute responses obtained by accounting for axial load effects for the set of ground motion records compatible with the spectrum of Fig. 7 a). Fig. 9-b compares the average response envelopes obtained by accounting for and by disregarding axial load effects.

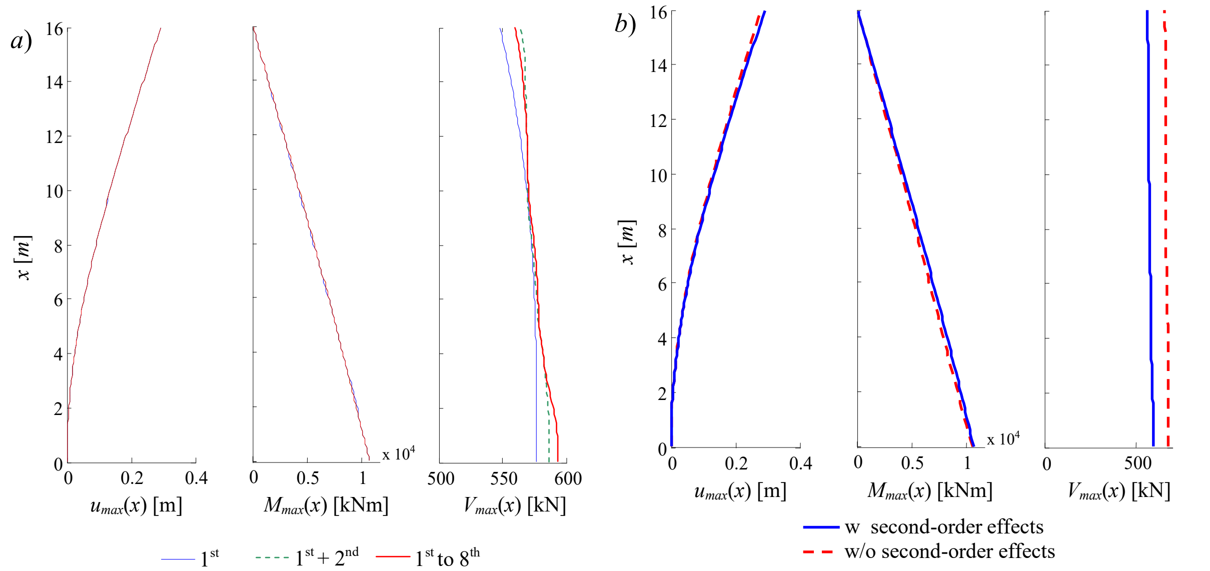

Fig. 9. Average seismic response of case study 2: a) modal contributions to the displacements, bending moments and shear, b) comparison between the response evaluated by accounting for and disregarding axial load effects.

The displacement demand for the pier is inferior to the yield limit of 0.3 m given in Wei et al. [26]; consequently, the elastic behaviour assumption is accurate for this system, despite the quite severe seismic input considered (PGA = 0.3g). In this application example, the contribution of higher vibration modes to the response is practically negligible for the displacement and the bending moment demand, and modest also for the shear demand (Fig. 9 a). This is related to the lower value of β for the case study 2 in comparison to that of the previous case study 1, which directly affects the importance of higher order modes due to the distributed pier mass.

The axial load effects influence only the shear demand (Fig. 9 b), and the value of the base shear reduces of about 17% when axial load effects are taken into account. This is explained again by the period elongation effect due to axial loads, which results in a reduction of the acceleration spectrum ordinates. The bending moments obtained by accounting for and by disregarding axial load effects are very similar. This can be justified in view of two counteracting effects related to axial loads: the bending moment reduction due to the decrease of spectral ordinates, and the increment of bending moment demand due to the vertical force at the pier top acting on the deformed configuration.

The base section bending moment demand, evaluated via first order analysis and amplified by the EC8-part 2 moment magnification factor [4] (i.e., 1401.5 kNm) is equal to 11898.3 kNm. The corresponding value evaluated with the proposed model is 10639.4 kNm. Thus, also in this case the EC8-Part 2 approach provides overconservative estimates of the effects of axial loads on the moment demand. The value of r_{MC}=1.11 is consistent with the value shown in Fig. 5-d of the parametric study of section 3.3 for $\alpha^2 = 0.163$ and $\beta = 0.141$.

4.3 Case study 3 (T_0=7s, $T_0/T_E \approx 1.4$)

This case study consists of a very tall bridge pier belonging to a regular multi-span bridge, whose properties are taken from Li et al. [35]. The pier is 90 m high and has a hollow square cross-section of dimensions 4.4 m x 4.4 m and thickness 0.5m. The longitudinal reinforcement ratio is 1.48%. The concrete has cylindrical mean strength of 48 MPa. The vertical force at the pier top transmitted by the deck is equal to 6867 kN. The pier cracked stiffness and distributed mass are respectively $b(x) = EI = 2.225\cdot 10^6$ kNm^2 and $m(x) = \bar{m} = 19.87$ ton/m, whereas the mass concentrated at the pier top is M_T = 700 ton. The values of the pier characteristic parameters are $\alpha^2 = P/P_{cr} = 0.101$, β = 2.556, and γ = 0.259. The value of the sum $\alpha^2+\gamma$ is equal to 0.36, denoting an higher slenderness of this pier with respect to the case studies previously analysed, characterized by lower $\alpha^2+\gamma$ values, of the order of 0.17. Moreover, the high value of β anticipates that, in this specific case, higher order modes are likely to contribute significantly to the response. The first three vibration periods of the pier disregarding axial load effects are 6.968 s, 0.884 s, and 0.292 s, whereas the corresponding values obtained by accounting for axial load effects are 7.692 s, 0.895 s, 0.293 s. In this case, also the higher modes vibration period are slightly influenced by axial load effects. The mass participation factors of the first three modes obtained by accounting for and by disregarding axial loads effects almost coincide and their values are 67.43%, 16.76%, and 5.46%. This also confirms that the second and third mode of vibration are expected to contribute significantly to the response.

Fig. 10a shows the average of the peak absolute responses obtained by accounting for axial load effects and by considering the different modal contributions. As expected, the higher modes of vibration dominate the pier seismic response. In particular, the second mode gives a significant contribution to the bending moment and shear demand. The value of the moment demand at x = 55m including the axial load effects is only slightly lower than the value at the pier base. Thus, plastic hinges are expected to form also at this location, as already observed in [35]. However, it should be pointed out that the pier responds elastically to the assumed seismic input and plastic hinges will form only for very severe excitations. In particular, plastic hinges were reported to form only for PGA values higher than 0.4g [35].

Fig. 10b compares the average response envelopes obtained by accounting for and by disregarding axial load effects. These effects have a negligible influence on the response. This is a consequence of the relevant contribution of higher modes, which are not significantly affected by axial load effects. Finally, it is worth noting that also in this case the EC8-Part 2 approach [4] gives conservative estimates of the effects of axial loads on the moment demand, with the increment equal to 1133.7 kNm. The r_{MC} ratio in this case is equal to 1.08, and it is consistent to the value r_{MC} = 1.05 obtained from the parametric study results shown in Fig. 5-f, for α^2 = 0.101 and β = 2.556.

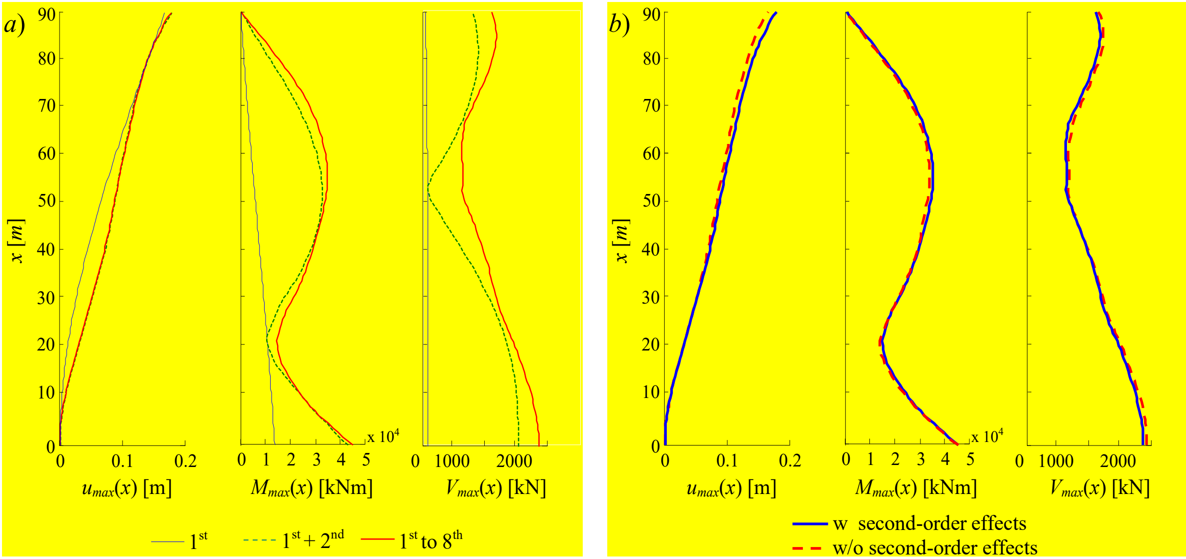

Fig. 10. Average seismic response of case study 3: a) modal contributions to the displacements, bending moments and shear, b) comparison between the responses evaluated by accounting for and by disregarding axial load effects.

5 CONCLUSIONS

The study performed in this paper aims to quantify the influence of both axial loads and higher order modes on the seismic response of tall piers, which are the most important components of the earthquake resisting system of bridges.

The analytical formulation validated in a previous study is herein adopted to analyse a wide range of piers and bridge configurations to provide a global overview of the problem. First, a thorough parametric investigation is carried out to evaluate how the system modal and seismic response is influenced by the main characteristic parameters. Afterwards, three realistic case studies, representative of different geometrical and dynamic conditions, are selected and seismic time-history analyses are performed to further investigate the influence of the aforesaid parameters.

Based on the results from both parametric investigation and case studies, the following general conclusions can be drawn.

Regarding the modal properties:

- the first period of vibration is the only one significantly affected by both axial loads and pier distributed mass;
- conversely, the first mode mass participation factor is not sensitive to the axial load, whereas the higher modes participation factors show significant variations.

Regarding the seismic response:

- the internal forces of the pier (i.e., shear and bending demand) are differently affected by the axial loads and higher order modes depending on the specific values assumed by the two main governing parameters, i.e., the pier top load intensity (governing the axial load effects) and the distributed mass (governing the contribution of higher order modes).

- The base shear reduces if the axial load effects are taken into account, and this effect can be very important in piers with low distributed mass values; however, this reduction may be compensated by the counteraction exerted by the higher order modes in case of piers with relatively large values of distributed mass.
- The bending moment response is similarly affected by axial loads and higher modes; in particular, the pier top load increment generates a decrease of the bending moment response, whereas the rise of the pier distributed mass compensates for this reduction and may also lead, in case of very long period systems, to an increment at the base of the pier.
- It is also worth mentioning that the bending moment reduction due to the decrease of spectral ordinates is often high enough to balance the increment of bending moment demand produced by the pier top vertical force acting on the deformed configuration.
- The shear and bending demand assessed neglecting higher modes contribution may be notably underestimated, in particular for piers with high fundamental period; more specifically, the second mode provides the highest contribution, while modes from 3 to 8 do not significantly affect the response.
- Moreover, in case of high distributed mass values and long period systems, a first mode-based estimation might be not adequate to correctly describe the internal actions distribution along the pier height, thus potential plastic region at locations different from the base of the pier might be not identified.
- From the case study analyses it can be concluded that at least the first two modes have to be considered to correctly estimate the shear and bending demand of tall piers.

Finally, with regard to the effectiveness of the simplified design approaches suggested by the Eurocode 8 to account for the second order effects, the following points deserve to be highlighted:

- the application of the EC8 design procedure to piers with low distributed mass brings to results extremely conservative and this trend increases with the pier top load intensity and system fundamental periods;
- conversely, the overestimation produced by the EC8 design procedure is lower in piers with high distributed mass and the conservativism of results reduces for smaller axial loads and with the system fundamental period;

- in all cases investigated, the amplification factors of EC8 are always from the safety side.

Due to the relevance of problem, it might be useful to extend the present study within a probabilistic framework aimed at characterizing the seismic response of tall piers beyond the design condition, by consequently removing the hypothesis of elastic response.

Moreover, given the observed sensitivity to the axial loads, future studies might be recommended to consider near-fault pulse-like ground motions, in particular aimed at exploring the influence of their relatively high vertical component of the excitation.

REFERENCES

[1] Kolias B. Overview of seismic issues for bridge design. In Athanasopoulou A, Poljansek M, Pinto A, Tsionis G, Denton S eds. *Workshop "Bridge Design to Eurocodes* 2010; Vienna, Austria. http://eurocodes.jrc.ec.europa.eu/showpage.php?id=334_1

[2] Mitoulis S.A. (2012). "The inefficacy of seismic isolation in bridges with tall piers", In Proc., 15th WCEE - World Conference on Earthquake Engineering, Lisbon, Portugal, paper No 3944.

[3] Mitoulis S.A. "Bridges with fixities and bearings vs isolated systems", COMPDYN 4th International Conference in Computational Methods in Structural Dynamics and Earthquake Engineering, Kos, Greece, 12-14 June 2013.

[4] European Committee for Standardization (ECS). *Eurocode 8: Design of structures for earthquake resistance*. European Committee for Standardization. Brussels, Belgium, 2005.

[5] AASHTO. LRFD bridge design specifications, 6th edition. Washington, DC; 2012.

[6] NTC18 – D.M. LL. PP. 17 Gennaio 2018. Aggiornamento delle «Norme tecniche per le costruzioni», 2018 (in Italian).

[7] Chen WF, Duan L. *Bridge Engineering. Seismic Design*. CRC Press LLC, New York, 2003.

[8] Shiravand MR, Rasouli M. Effects of substructure mass participation on natural period of multi-column base isolated bridges. *Structures* 2019; **20**: 88-104.

[9] Chen, X., & Li, C. (2020). Seismic performance of tall pier bridges retrofitted with lead rubber bearings and rocking foundation. *Engineering Structures*, 212, 110529. DOI: 10.1016/j.engstruct.2020.110529

[10] Chen, X., Xiang, N., & Li, C. (2021). Influence of higher-order modes of slender tall pier bridge columns on the seismic performance of pile foundations. Soil Dynamics and Earthquake Engineering, 142, 106543. DOI: 10.1016/j.soildyn.2020.106543

[11] Chen X, Guan Z., Spencer Jr BF, Li J. A simplified procedure for estimating nonlinear seismic demand of tall piers. *Engineering Structures* 2018; **174**: 778-791.

[12] Chen X, Guan Z, Li J, Spencer Jr BF. Shake table tests of tall-pier bridges to evaluate seismic performance. *Journal of Bridge Engineering* 2018; **23**(9): 04018058.

[13] Liu Y, Mei Z, Wu B, Bursi OS, Dai KS, Li B, Lu Y. Seismic behaviour and failure-mode-prediction method of a reinforced-concrete rigid-frame bridge with thin-walled tall piers: Investigation by model-updating hybrid test. *Engineering Structures* 2020; **208**: 110302.

[14] Mei Z, Wu B, Bursi OS, Xu G, Wang Z, Wang T, Ning X, Liu Y. Hybrid simulation with online model updating: Application to a reinforced concrete bridge endowed with tall piers. *Mechanical Systems and Signal Processing* 2019; **123**: 533-553.

[15] Tubaldi E, Tassotti L, Dall'Asta A, Dezi L. Seismic response analysis of slender bridge piers. *Earthquake Engineering and Structural Dynamics* 2014; **43**: 1503-1519.

[16] Guan Z, Li J, Xu Y, Lu H. Higher-order mode effects on the seismic performance of tall piers. *Frontiers of Architecture and Civil Engineering in China* 2011; **5**(4): 496–502.

[17] Ceravolo R, Demarie GV, Giordano L, Mancini G, Sabia D. Problems in applying code-specified capacity design procedures to seismic design of tall piers. *Engineering Structures* 2009; **31**(8): 1811–1821.

[18] Dhakal RP, Maekawa K. Analytical Prediction of Collapse of RC Piers Induced by Geometrical Nonlinearity. *The First International Conference on Structural Stability and Dynamics* 2000; Taipei, Taiwan.

[19] Kwak HG, Kim JK. Effect of slender RC columns under seismic load. *Engineering Structures* 2007; **29**(11): 3121–3133.

[20] Virgin LN. *Vibration of axially loaded structures*. Cambridge University press, 2007.

[21] Bernal D. Amplification factors for inelastic dynamic p–Δ effects in earthquake analysis. *Earthquake Engineering & Structural Dynamics* 1987; **15**(5): 635–651.

[22] Mahin S, Boroschek R. *Influence of geometric nonlinearities on the seismic response and design of bridge structures*. Background report to California Department of Transportation, 1991.

[23] Fenwick RC, Davidson BJ, Chung BT. P - delta actions in seismic resistant structures. *Bulletin of the New Zealand National Society for Earthquake Engineering* 1992; **25**(1): 56–69.

[24] MacRae GA. P-Δ effect on single-degree-of-freedom structures in earthquakes. *Earthquake Spectra* 1994; **10**(3): 539–568.

[25] Priestley MJN, Calvi GM, Kowalsky MJ. *Displacement-based seismic design of structures*. IUSS Press: Pavia, Italy, 2007.

[26] Wei B, Xu Y, Li J. Treatment of P-Δ Effects in Displacement-Based Seismic Design for SDOF Systems. *Journal of Bridge Engineering* 2012; **17**(3): 509–518.

[27] Chen X, Li J, Guan Z. Fragility analysis of tall pier bridges subjected to near-fault pulse-like ground motions. *Structure and Infrastructure Engineering* 2019; 1-14, DOI: 10.1080/15732479.2019.1683589.

[28] Chen X. System Fragility Assessment of Tall-Pier Bridges Subjected to Near-Fault Ground Motions. *Journal of Bridge Engineering* 2020; **25**(3): 04019143.

[29] Rao SS. *Vibration of Continuous Systems*. Wiley: New York, 2007.

[30] Tubaldi E, Dall'Asta A. Transverse free vibrations of continuous bridges with abutment restraint. *Earthquake Engineering & Structural Dynamics* 2012; **41**(9): 1319–1340.

[31] Naguleswaran S. Transverse vibration of an uniform Euler–Bernoulli beam under linearly varying axial force. *Journal of Sound and Vibration* 2004, **275**(1-2): 47–57.

[32] Chopra AK. *Dynamics of structures: Theory and Applications to Earthquake Engineering*. Prentice - Hall Inc., 1995.

[33] Wilson, E. L. *Three-dimensional static and dynamic analysis of structures*, Computers and Structures, Inc., 2002.

[34] Smerzini C, Galasso C, Iervolino I, Paolucci R. Ground motion record selection based on broadband spectral compatibility. Earthquake Spectra 2013; **30**(4): 1427-1448.

[35] Li JZ, Liang ZY, Jiao CY. Investigation on rational analytical model of tall bridge pier, Proceedings of the 14th World Conference on Earthquake Engineering 2008; October 12-17 2008, Beijing, China.